

## *N*-(3-Cyano-4,5,6,7-tetrahydro-1-benzothien-2-yl)amides as potent, selective, inhibitors of JNK2 and JNK3

Richard M. Angell,<sup>a,†</sup> Francis L. Atkinson,<sup>a</sup> Murray J. Brown,<sup>b</sup> Tsu Tshen Chuang,<sup>b</sup> John A. Christopher,<sup>a,\*</sup> Maria Cichy-Knight,<sup>c</sup> Allison K. Dunn,<sup>c</sup> Kendra E. Hightower,<sup>d</sup> Susanna Malkakorpi,<sup>a</sup> James R. Musgrave,<sup>b</sup> Margarete Neu,<sup>a</sup> Paul Rowland,<sup>b</sup> Robyn L. Shea,<sup>a</sup> Jeffery L. Smith,<sup>d</sup> Donald O. Somers,<sup>a</sup> Sonia A. Thomas,<sup>c</sup> Gladstone Thompson<sup>a</sup> and Ruolan Wang<sup>d</sup>

<sup>a</sup>GlaxoSmithKline R&D, Medicines Research Centre, Gunnels Wood Road, Stevenage, Hertfordshire SG1 2NY, UK

<sup>b</sup>GlaxoSmithKline R&D, New Frontiers Science Park, Third Avenue, Harlow, Essex CM19 5AW, UK

<sup>c</sup>GlaxoSmithKline Inc., 1250 South Collegeville Road, Collegeville, PA 19426, USA

<sup>d</sup>GlaxoSmithKline Inc., 5 Moore Drive, Research Triangle Park, NC 27709, USA

Received 7 November 2006; revised 1 December 2006; accepted 3 December 2006

Available online 15 December 2006

**Abstract**—The identification and exploration of a novel, potent and selective series of *N*-(3-cyano-4,5,6,7-tetrahydro-1-benzothien-2-yl)amide inhibitors of JNK2 and JNK3 kinases is described. Compounds **5a** and **11a** were identified as potent inhibitors of JNK3 (pIC<sub>50</sub> 6.7 and 6.6, respectively), with essentially equal potency against JNK2 (pIC<sub>50</sub> 6.5). Selectivity within the mitogen-activated protein kinase (MAPK) family, against JNK1, p38 $\alpha$  and ERK2, was observed for the series. X-ray crystallography of **5e** and **8a** in JNK3 revealed a unique binding mode, with the 3-cyano substituent forming an H-bond acceptor interaction with the hinge region of the ATP-binding site.

© 2006 Elsevier Ltd. All rights reserved.

Protein kinases catalyse the phosphorylation of tyrosine and serine/threonine residues in proteins involved in the regulation of diverse cellular functions. Aberrant kinase activity is implicated in many diseases, which makes the inhibition of kinases an attractive target for the pharmaceutical industry.<sup>1</sup>

The mitogen-activated protein kinase (MAPK) pathways comprise a major signalling system used to transduce extracellular signals to intracellular responses. The MAPK family of serine-threonine protein kinases consists of the extracellular-regulated protein kinases (ERK), p38 mitogen-activated kinases (p38 MAPK) and the *c-Jun* N-terminal kinases (JNK).<sup>2</sup>

The JNK kinases are implicated in several disease areas, including neurodegeneration, rheumatoid arthritis,

inflammatory disorders, cancer and diabetes.<sup>3,4</sup> They differ in their tissue expression profile and functions, with JNK1 and JNK2 being widely expressed, whereas JNK3 is expressed predominantly in the brain and at lower levels in the heart and testis.<sup>5,6</sup> JNK3 appears to play important roles in the brain to mediate neurodegeneration, such as beta amyloid processing, Tau phosphorylation and neuronal apoptosis in Alzheimer's Disease, as well as the mediation of neurotoxicity in a rodent model of Parkinson's Disease.<sup>7,8</sup> Identifying potent inhibitors of JNK3, with selectivity within the wider MAPK family, may contribute towards neuropro-

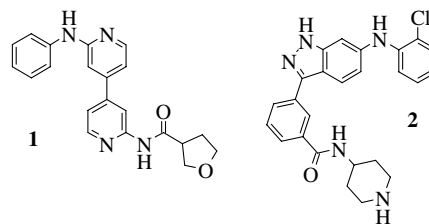


**Figure 1.** Selective JNK3 inhibitors **1** and **2**.

**Keywords:** Kinase; Inhibitor; JNK; JNK3; MAPK; Selective.

\* Corresponding author. Tel.: +44(0)1438 763578; e-mail:

[John.A.Christopher@gsk.com](mailto:John.A.Christopher@gsk.com)

† Present address: Arrow Therapeutics Ltd, Britannia House, 7 Trinity Street, London SE1 1DB, UK.

tection therapies with reduced side effect risks, and will aid the further understanding of the roles of the individual JNK kinases.

The amino acid sequence identity of the JNK kinases is greater than 90%, with >98% homology within the ATP-binding site. To date, few reports of inhibitor series with significant selectivity within the JNK family have been published, recent examples of JNK3 selective inhibitors being 2'-anilino-4,4'-bipyridines and 6-anilinoindazoles, such as compounds **1** and **2**, respectively (Fig. 1).<sup>9,10</sup>

A screening exercise led to the identification of *N*-(3-cyano-4,5,6,7-tetrahydro-1-benzothien-2-yl)amides such as **3**, Figure 2, with good JNK3 inhibitory activity in a binding assay.<sup>11</sup>

In order to explore the structure–activity relationships (SAR) at the 2-position, we embarked upon the synthesis of analogues of **3** using procedures illustrated in Scheme 1. Amine **4** was prepared from cyclohexanone, sulfur and malononitrile under conditions reported by Gewald, followed by formation of amides, ureas or sulfonamides under standard conditions.<sup>12</sup>

The JNK1, JNK3 and p38 $\alpha$  inhibitory activity of compounds **5a–5n** was evaluated (Table 1).<sup>13</sup> Clear SAR

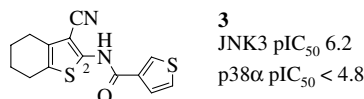
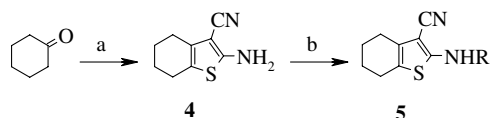


Figure 2. Hit compound **3**.



**Scheme 1.** Reagents and conditions: (a) malononitrile, sulfur, Et<sub>2</sub>NH, EtOH, rt; (b) acid chloride, pyridine, 80 °C or isocyanate, DMF/pyridine (1:1), rt or sulfonyl chloride, 4-pyrrolidinopyridine, diisopropylethylamine, CH<sub>2</sub>Cl<sub>2</sub>/pyridine (1:1).

Table 1. JNK1, JNK3 and p38 $\alpha$  inhibition of **5a–n**, values in pIC<sub>50</sub>

Compound	R	JNK1	JNK3	p38 $\alpha$
<b>5a</b>	–C(O)(1-naphthyl)	<5.0	6.7	<4.8
<b>5b</b>	–C(O)(4-F-1-naphthyl)	<5.0	6.0	<4.8
<b>5c</b>	–C(O)phenyl	<5.0	5.8	<4.8
<b>5d</b>	–C(O)(4-F-phenyl)	<5.0	5.5	<4.8
<b>5e</b>	–C(O)(2-F-phenyl)	<5.0	6.4	<4.8
<b>5f</b>	–C(O)(2-Br-phenyl)	<5.5	5.5	<4.8
<b>5g</b>	–C(O)CH <sub>2</sub> phenyl	<5.0	<4.8	<4.8
<b>5h</b>	–C(O)CH <sub>2</sub> (2-Br-phenyl)	ND <sup>a</sup>	<4.8	<4.8
<b>5i</b>	–C(O)CH <sub>2</sub> (4-morpholine)	ND	<4.8	<4.8
<b>5j</b>	–C(O)cyclohexyl	ND	<4.8	<4.8
<b>5k</b>	–SO <sub>2</sub> (1-naphthyl)	ND	<4.8	<4.8
<b>5l</b>	–C(O)NH(1-naphthyl)	ND	<4.8	<4.8
<b>5m</b>	–C(O)NH(cyclopentyl)	ND	<4.8	<4.8
<b>5n</b>	–SO <sub>2</sub> (3-Me-phenyl)	ND	<4.8	<4.8

<sup>a</sup> ND, not determined.

emerged; amides with aryl substituents (**5a–5f**) were tolerated, whereas those with benzyl, alkyl or cycloalkyl substituents (**5g–j**) were not. Sulfonamide **5k** and urea **5l** (direct analogues of amide **5a**) were also inactive, as were further examples of ureas and sulfonamides, including **5m** and **5n**.

Significant selectivity for JNK3 over JNK1 was observed; selectivity within the JNK family being an unexpected and noteworthy feature of the series. Two examples, **5a** and **5b**, were also evaluated in an ERK2 kinase assay, and were found to be inactive, which together with the inactivity of all compounds against p38 $\alpha$  indicates a high degree of selectivity for the series within the wider MAPK family.<sup>14</sup>

In order to understand the observed activity and selectivity, and to guide further medicinal chemistry efforts, a crystal structure of **5e** complexed with JNK3 (at 2.45 Å resolution) was obtained, which revealed several interesting features (Fig. 3).<sup>15</sup>

First, the crystal structure revealed that the conserved hydrogen bond from the hinge backbone amide NH (of Met149 in JNK3) is accepted by the 3-cyano substituent of **5e**.<sup>17</sup> Although there is ample crystallographic, physicochemical and theoretical evidence that the nitrile group is a reasonably strong hydrogen-bond acceptor, there are few examples where it is known to act as the conserved acceptor in a kinase ligand: a notable recent example is a 5-cyanopyrimidine inhibitor of p38 $\alpha$ .<sup>18–21</sup> Another unusual feature of the structure is the donation of a hydrogen bond from the amide nitrogen to the sulfur of Met146, with a distance of 3.65 Å between the nitrogen and sulfur atoms. This rare, though not unprecedented, interaction may contribute to the good selectivity profile of these compounds, as the H-bonding valency of the NH might otherwise go unsatisfied.<sup>22,23</sup> The amide

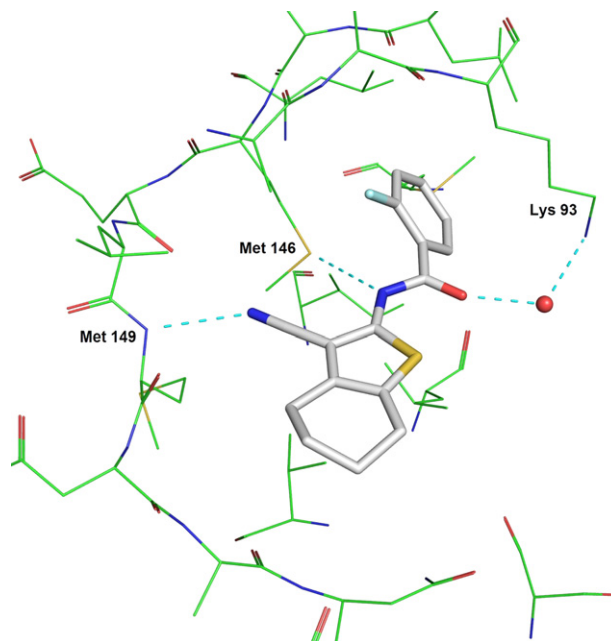


Figure 3. Crystal structure of **5e** in the JNK3 ATP-binding site.

oxygen is hydrogen-bonded, via a bridging water, to the conserved Lys93.

The 2-(2-fluoro)benzamide substituent occupies an ‘induced-fit’ hydrophobic pocket at the back of the active site (Hydrophobic Region I in the nomenclature of Traxler et al.) which is formed mainly by the sidechains of Val78, Ala91, Lys93, Met115, Ile124, Leu126, Leu144, Met146 and Leu206 and is exposed by the rearrangement of the ‘gatekeeper’ Met146.<sup>10,17,24,25</sup>

The steric complementarity between the aromatic substituent of **5e** and the pocket is generally very good. We believe this feature to be an important determinant of the potency and specificity of the series, and helps to explain the effects on JNK3 potency shown in Table 1. For example, the homologated (**5g**) and saturated (**5j**) analogues of phenyl amide **5c** are inactive, indicating the limited extent of the pocket. More subtly, the 2-fluorophenyl compound **5e** is around fivefold more potent than the parent **5c**, whereas the 4-fluorophenyl and 4-fluoronaphthyl analogues **5d** and **5b** are *less* potent than the parent phenyl and naphthyl amides (**5c** and **5a**, respectively). The pocket is somewhat open towards the C-terminal lobe (i.e., in the 5- and 6-positions of the phenyl ring of **5e**), and this led us to believe it could be beneficial to extend the ligand in this region. The 1-naphthyl analogue **5a** tests this hypothesis and is indeed an order of magnitude more potent than **5c**.

The induced-fit pocket contains the only active-site residue that differs between JNK3 and JNK1, Leu144 in the former corresponding to Ile106 in the latter. It is likely that the difference in the shape of the pocket thus introduced contributes to the reduced potency vs. JNK1 (although other factors, such as differences in lobe orientation, could also contribute). This hypothesis is in agreement with that proposed by Swahn to explain the JNK3 selectivity of bipyridines such as **1**.<sup>10</sup>

The residues that comprise the pocket in JNK3 are largely conserved in p38 $\alpha$ , a notable exception being the gatekeeper, which is Thr106 in p38 $\alpha$ . Despite these similarities, inspection of the structure of **5e** and of comparable p38 $\alpha$  crystal structures suggests that there are considerable differences in the shape of the pocket, due to, for example, differences in domain orientation.<sup>25</sup>

This, alongside the differing gatekeeper and differences in the hinge region, means the lack of p38 $\alpha$  activity can be understood.

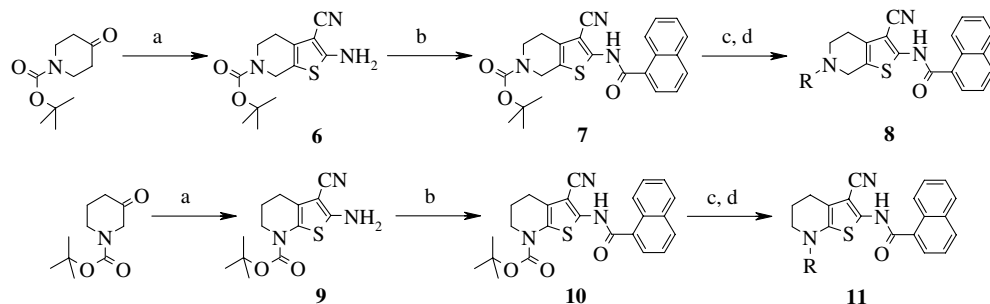
The gatekeeper residue in ERK2 is Gln103, which does not undergo the rearrangement observed for Met146 in JNK3, and this kinase is believed to be relatively insensitive to back-pocket binding ligands.<sup>26</sup> The lack of ERK2 inhibitory activity of **5a** and **5b** (and as discussed below, **8a–c**, **11a–e**) was thus expected.

Guided by the X-ray structure of **5e**, another iteration of medicinal chemistry was embarked upon, which sought to expand the diversity of the template by incorporating a second point of substitution. From the structure, it appeared likely that space was available within the active site to allow substitution at the 6- or 7-positions of the tetrahydrobenzothiophene ring. It is believed that this could be beneficial as additional, favourable, interactions within the active site could be made, or egress from the active site into the solvent front region could allow moderation of the solubility and lipophilicity of the series, without detriment to enzyme activity or selectivity. Definitive SAR data to support the attainment of these goals are not reported in this communication.

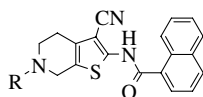
Modification of the original route readily allowed access to key intermediates **6** and **9** from 1-Boc-4-piperidone and 1-Boc-3-piperidone, respectively, as depicted in Scheme 2. These could then be progressed through a sequence of acylation, Boc-cleavage and N-substitution to yield amides, amines or sulfonamides **8a–c** and **11a–e**.

As illustrated in Tables 2 and 3, respectively, introduction of a 6- or 7-substituent maintained the selectivity previously observed for JNK3 over JNK1 and p38 $\alpha$ . The selectivity over ERK2 observed for **5a** and **5b** was also maintained. In general, substitution at the 7-position was more profitable than at the 6-position, a variety of amide, sulfonamide and amine substitutions being tolerated, with inhibition values in excess of pIC<sub>50</sub> 6 readily attained. Substitution at the 6-position was less beneficial, amides **8a** and **8b** and sulfonamide **8c** being only moderately active.

A crystal structure in JNK3 was obtained of **8a** (at 2.10 Å resolution), revealing an identical binding mode to that

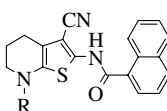


**Scheme 2.** Reagents and conditions: (a) malononitrile, sulfur, Et<sub>2</sub>NH, EtOH, rt; (b) 1-naphthylcarbonyl chloride, pyridine, 80 °C; (c) HCl/Dioxane (1:10), 80 °C; (d) Sulfonyl chloride, pyridine, CH<sub>2</sub>Cl<sub>2</sub>, rt or carboxylic acid, polymer-supported carbodiimide, 4-dimethylaminopyridine, CH<sub>2</sub>Cl<sub>2</sub>, reflux or aldehyde, 3 Å molecular sieves, CH<sub>2</sub>Cl<sub>2</sub>/AcOH (100:1), 40 °C then NaBH(OAc)<sub>3</sub>, rt.

**Table 2.** JNK1, JNK3, p38 $\alpha$  and ERK2 inhibition of **8a–8c**, values in pIC<sub>50</sub>

Compound	R	JNK1	JNK3	p38 $\alpha$	ERK2
<b>8a</b>	–C(O)(CH <sub>2</sub> ) <sub>2</sub> (1-piperidine)	<5.0	5.5	<4.8	<5.0
<b>8b</b>	–C(O)CH <sub>2</sub> NMe <sub>2</sub>	<5.0	5.6	<4.8	<5.0
<b>8c</b>	–SO <sub>2</sub> phenyl	<5.0	5.5	<4.8	<5.0

Modifications at the 6-position.

**Table 3.** JNK1, JNK3, p38 $\alpha$  and ERK2 inhibition of **11a–11e**, values in pIC<sub>50</sub>

Compound	R	JNK1	JNK3	p38 $\alpha$	ERK2
<b>11a</b>	–C(O)cyclopropyl	<5.0	6.6	<4.8	<5.0
<b>11b</b>	–C(O)(1 <i>H</i> -pyrazol-3-yl)	<5.0	6.6	<4.8	<5.0
<b>11c</b>	–CH <sub>2</sub> (4-SO <sub>2</sub> Me-phenyl)	<5.0	6.0	<4.8	<5.0
<b>11d</b>	–CH <sub>2</sub> (3-pyridyl)	<5.0	6.3	<4.8	<5.0
<b>11e</b>	–SO <sub>2</sub> phenyl	<5.0	5.8	<4.8	<5.0

Modifications at the 7-position.

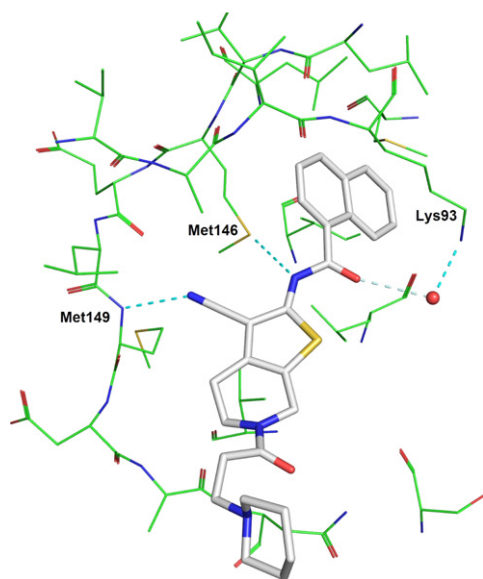
observed for **5e** (Fig. 4).<sup>15</sup> The structure showed that, as expected, the piperidine portion of the 6-amide substituent accesses the solvent front, and that the naphthyl substituent adopts an analogous orientation to the 2-fluorophenyl portion of **5e**.

Extensive profiling of the series (data not shown) revealed that the selectivity observed for JNK3 over JNK1, p38 $\alpha$  and ERK2 is matched by an outstanding

overall kinase selectivity profile, which appears to be intrinsic to the template rather than a function of appropriate pendant functionality. For example, **5a** and **11a** were screened in a panel of more than 30 kinase assays, including Alk5, c-Fms, CDK-2, EGFR, ErbB2, GSK3 $\beta$ , PLK1, Src, Tie-2 and VegFr2, and were inactive (pIC<sub>50</sub> < 5.0) against all of them. In addition, **5c** was submitted to the Kinomescan assay panel of over 200 kinases (Ambit Biosciences), which utilise kinases or kinase domains fused to T7 bacteriophage.<sup>27</sup> The compound only showed significant ability to displace an immobilised ATP-site ligand from JNK3.

To understand the full picture of selectivity within the JNK family, the JNK2 inhibitory activities of key compounds **5a**, **8a** and **11a** were assessed.<sup>28</sup> The data obtained (pIC<sub>50</sub> 6.5, 5.3 and 6.5, respectively) indicate that the series does not have significant selectivity for JNK3 over JNK2. Only one residue differs in the active sites; Met115 in JNK3 corresponds to Leu77 in JNK2. This residue is peripheral, and thus it would not be expected to impact inhibitor binding.

In summary, *N*-(3-cyano-4,5,6,7-tetrahydro-1-benzothien-2-yl)amides, and variants with additional substitution in the tetrahydrobenzene ring, represent a potent, selective series of JNK kinase inhibitors. The excellent intrinsic selectivity for JNK3/JNK2 over JNK1, and within the MAPK family, coupled with the unique binding mode via the nitrile interaction with the backbone, represent key features of the series. A second point of diversity introduced by a nitrogen at the 7-position

**Figure 4.** Crystal structure of **8a** in the JNK3 ATP-binding site.

provides a focus for future investigation, preferred over the 6-position based on target affinity.

### Acknowledgments

David Brown, Emma Mackenzie, Yvonne Joseph, Isabelle Davis and the GSK Screening and Compound Profiling group are gratefully acknowledged for the generation of kinase inhibition data. The authors also thank Karen Lackey and David Miller for their guidance and support, Paul Bamborough for proof-reading the manuscript, and Terry Panchal and Mark Bamford for useful discussions.

### References and notes

- Parang, K.; Sun, G. *Curr. Opin. Drug Disc. Dev.* **2004**, *7*, 617.
- Herlaar, E.; Brown, Z. *Mol. Med. Today* **1999**, *5*, 439.
- Manning, A. M.; Davis, R. J. *Nat. Rev. Drug Disc.* **2003**, *2*, 554.
- Liu, G.; Rondinone, C. M. *Curr. Opin. Investig. Drugs* **2005**, *6*, 979.
- Kuan, C.-Y.; Yang, D. D.; Roy, D. R. S.; Davis, R. J.; Rakic, P.; Flavell, R. A. *Neuron* **1999**, *22*, 667.
- Martin, J. H.; Mohit, A. A.; Miller, C. A. *Mol. Brain Res.* **1996**, *35*, 47.
- Resnick, L.; Fennell, M. *Drug Discovery Today* **2004**, *9*, 932.
- Kimberly, W. T.; Zheng, J. B.; Town, T.; Flavell, R. A.; Selkoe, D. J. *J. Neurosci.* **2005**, *25*, 5533.
- Swahn, B.-M.; Huerta, F.; Kallin, E.; Malmström, J.; Weigelt, T.; Viklund, J.; Womack, P.; Xue, Y.; Öhberg, L. *Bioorg. Med. Chem. Lett.* **2005**, *15*, 5095.
- Swahn, B.-M.; Xue, Y.; Arzel, E.; Kallin, E.; Magnus, A.; Plobeck, N.; Viklund, J. *Bioorg. Med. Chem. Lett.* **2006**, *16*, 1397.
- $pIC_{50} = -\log_{10} IC_{50}$ ; where  $IC_{50}$  is the concentration of compound required to inhibit the kinase activity by 50%. JNK3 kinase inhibitory activity was determined using a fluorescence anisotropy kinase binding assay. The kinase, a fluorescently labelled inhibitor and a variable concentration of test compound are incubated together to reach thermodynamic equilibrium under conditions such that in the absence of test compound the fluorescent inhibitor is significantly (>50%) enzyme bound and in the presence of a sufficient concentration ( $>10 \times K_i$ , where  $K_i$  = dissociation constant for inhibitor binding) of a potent inhibitor the anisotropy of the unbound fluorescent ligand is measurably different from the bound value. Truncated human JNK3 was expressed in baculovirus as a N-terminal His (6)-tagged fusion protein. This enzyme (JNK3) was activated in 50 mM Tris/HCl, pH 7.5, 0.1 mM EGTA, 0.1%  $\beta$ -mercaptoethanol, 0.1 mM sodium vanadate, 10 mM magnesium acetate, 0.1 mM ATP with 100 nM active MKK4 and MKK7 $\beta$  at 30 °C for 30 min. Following activation, the JNK3 was purified by Ni-NTA agarose chromatography. The JNK3 was then dialyzed into storage buffer (50 mM Tris/HCl, pH 7.5, 270 mM Sucrose, 150 mM NaCl, 0.1 mM EGTA, 0.1%  $\beta$ -mercaptoethanol, 0.03% Brij-35, 1 mM benzamidine and 0.2 mM PMSF), snap frozen in liquid nitrogen and stored at -70 °C. Inhibitor binding to JNK3 was assessed by a fluorescence anisotropy competitive binding assay. All components are dissolved in buffer of composition 50 mM Hepes, pH 7.5, 1 mM CHAPS, 1 mM DTT, 10 mM MgCl<sub>2</sub> with final concentrations of 10 nM JNK3 and 2 nM of a fluorescently labelled inhibitor. This reaction mixture is added to wells containing various concentrations of test compound (0.28 nM–16.6  $\mu$ M final) or DMSO vehicle (<3% final) in black 384-well microtitre plates and equilibrated for 30–300 min at room temperature to reach equilibrium. Fluorescence anisotropy is read in Molecular Devices Acquest (excitation 530 nm/emission 580 nm). The error of the assay is estimated as  $\pm 0.2$  log units, based on the median standard deviation of all compounds which have been tested more than eight times and have a mean  $pIC_{50} > 6$ . Under the assay conditions used to generate the data presented in this manuscript, the anthrapyrazolone JNK inhibitor SP600125 displayed inhibitory potencies of  $pIC_{50}$  6.4, 5.9 and <4.8 for JNK1, JNK3 and p38 $\alpha$ , respectively, in line with literature reports, see: Bennett, B. L.; Sasaki, D. T.; Murray, B. W.; O'Leary, E. C.; Sakata, S. T.; Xu, W.; Leisten, J. C.; Motiwala, A.; Pierce, S.; Satoh, Y.; Bhagwat, S. S.; Manning, A. M.; Anderson, D. W. *Proc. Natl. Acad. Sci. U.S.A.* **2001**, *98*, 13681.
- Gewald, K. *Chem. Ber.* **1965**, *98*, 3571.
- JNK1 kinase inhibitory activity was determined in an analogous fashion to that described above for JNK3, using recombinant full length human JNK1 $\alpha$ 1 L26318 (GenBank) expressed in baculovirus as an N-terminal His (6)-tagged fusion protein, and purified as above.<sup>11</sup> p38 $\alpha$  inhibitory activity data were generated using conditions previously described, see: Barker, M. D.; Hamblin, J. N.; Jones, K. L.; Patel, V. K.; Swanson, S.; Walker, A. L. Int. Patent Appl. WO 05/073232.
- ERK2 kinase inhibitory activity was determined in a similar fashion to that described above for JNK3, using recombinant full length ERK2 expressed and purified as previously described, see: McDonald, O. B.; Chen, W. J.; Ellis, B.; Hoffman, C.; Overton, L.; Rink, M.; Smith, A.; Marshall, C. J.; Wood, E. R. *Anal. Biochem.* **1999**, *268*, 318. The ERK2 used for the work described in this paper was not activated before or during the assay.
- Truncated JNK3 (residues 39–402, JNK3t) was prepared according to published conditions.<sup>16</sup> Cocrystals of JNK3t+AMP-PNP/Mg<sup>2+</sup> were obtained from JNK3t at 10 mg/ml with 2 mM MgCl<sub>2</sub> and 1 mM AMP-PNP. The crystals were grown at 10 °C, using the hanging drop vapour diffusion method, with a reservoir solution of 50 mM Tris/HCl, pH 7.2–7.6, 18–22% PEG3350 and 0.2 M KF and 1  $\mu$ l + 1  $\mu$ l hanging drops. JNK3t+MgAMP-PNP cocrystals were soaked at 20 °C in 50 mM Tris/HCl, pH 7.5, 20% PEG3350, and 0.2 M KF containing 0.8 mM inhibitor **5e** for 4 days. The **8a** complex was obtained in a similar way though crystals were soaked for 1 day in buffer (10  $\mu$ L) containing 0.1 mg of solid **8a** with 1 mM EDTA. Each crystal was cryoprotected by brief immersion into paratone-N (Hampton Research) prior to data collection. The PDB deposition codes for the **5e** and **8a** JNK3 complex crystal structures are 2O2U and 2O0U, respectively.
- Xie, X.; Gu, Y.; Fox, T.; Coll, J. T.; Fleming, M. A.; Markland, W.; Caron, P. R.; Wilson, K. P.; Su, M. S.-S. *Structure* **1998**, *6*, 983.
- Adams, J. L.; Veal, J.; Shewchuk, L. In *Protein Crystallography in Drug Discovery*; Babine, R. E., Abdel-Meguid, S. S., Eds.; Wiley-VCH: Weinheim, 2004, Chapter 2.
- Bruno, I. J.; Cole, J. C.; Lommerse, J. P. M.; Rowland, R. S.; Taylor, R.; Verdonk, M. L. *J. Comput. Aided Mol. Des.* **1997**, *11*, 525.
- Abraham, M. H. *Chem. Soc. Rev.* **1993**, *22*, 73.

20. Le Questel, J.-Y.; Berthelot, M.; Laurence, C. *J. Phys. Org. Chem.* **2000**, *13*, 347.
21. Liu, C.; Wroblewski, S. T.; Lin, J.; Ahmed, G.; Metzger, A.; Wityak, J.; Gillooly, K. M.; Shuster, D. J.; McIntyre, K. W.; Pitt, S.; Shen, D. R.; Zhang, R. F.; Zhang, H.; Doweiko, A. M.; Diller, D.; Henderson, I.; Barrish, J. C.; Dodd, J. H.; Schieven, G. L.; Leftheris, K. *J. Med. Chem.* **2005**, *48*, 6261.
22. Allen, F. H.; Bird, C. M.; Rowland, R. S.; Raithby, P. R. *Acta Crystallogr., Sect. B* **1997**, *B53*, 696.
23. Wennmohs, F.; Staemmler, V.; Schindler, M. *J. Chem. Phys.* **2003**, *119*, 3208.
24. Traxler, P.; Furet, P. *Pharmacol. Ther.* **1999**, *82*, 195.
25. Scapin, G.; Patel, S. B.; Lisnock, J.; Becker, J. W.; LoGrasso, P. V. *Chem. Biol.* **2003**, *10*, 705.
26. Wang, Z.; Canagarajah, B. J.; Boehm, J. C.; Kassisa, S.; Cobb, M. H.; Young, P. R.; Abdel-Meguid, S.; Adams, J. L.; Goldsmith, E. J. *Structure* **1998**, *6*, 1117.
27. The ability of **5c** at 10  $\mu$ M concentration to displace the fusion protein from immobilised ATP-site probe ligands was determined as previously described, see: Fabian, M. A.; Biggs, W. H., III; Treiber, D. K.; Atteridge, C. E.; Azimioara, M. D.; Benedetti, M. G.; Carter, T. A.; Ciceri, P.; Edeen, P. T.; Floyd, M.; Ford, J. M.; Galvin, M.; Gerlach, J. L.; Grotzfeld, R. M.; Herrgard, S.; Insko, D. E.; Insko, M. A.; Lai, A. G.; Lélías, J.-M.; Mehta, S. A.; Milanov, Z. V.; Velasco, A. M.; Wodicka, L. M.; Patel, H. K.; Zarrinkar, P. P.; Lockhart, D. J. *Nat. Biotechnol.* **2005**, *23*, 329.
28. JNK2 data were obtained in a radiometric filter binding assay, using human JNK2 $\alpha$ 2 with ATF2 as substrate, in the presence of [ $\gamma$ - $^{33}$ P]ATP (45  $\mu$ M). For further details, see: [www.upstate.com](http://www.upstate.com).